

Multiple acoustic surface plasmons in graphene/Cu(111) contacts

A. Politano,^{1,*} H. K. Yu,² D. Farías,³ and G. Chiarello^{4,†}

¹*Fondazione Istituto Italiano di Tecnologia, Graphene Labs, Via Morego 30, 16163 Genova, Italy*

²*Department of Materials Science and Engineering and Department of Energy Systems Research, Ajou University, Suwon 16499, Korea*

³*Departamento de Física de la Materia Condensada; Instituto “Nicolás Cabrera”; Condensed Matter Physics Center (IFIMAC); Universidad Autónoma de Madrid, 28049 Madrid, Spain*

⁴*Dipartimento di Fisica, Università della Calabria, 87036 Rende, Cosenza, Italy*



(Received 27 September 2017; revised manuscript received 31 October 2017; published 11 January 2018)

The excitation spectrum of graphene on Cu(111), probed by momentum-resolved electron-energy-loss spectroscopy, exhibits multiple acoustic surface plasmons (ASP), arising from both the graphene overlayer and the Cu(111) substrate. We have investigated the mutual interaction between the ASP of the graphene overlayer and that of the underlying Cu(111) substrate. The weak interaction between graphene and Cu(111) implies that the ASP of Cu(111) survives, with only slight changes in its group velocity. Remarkably, we find that the damping processes of ASP are mitigated as compared to the cases of other graphene/metal interfaces. Therefore, this interface is an ideal graphene/metal contact for graphene-based plasmonics. Moreover, the presence of graphene coating protects the ASP of Cu(111) from quenching in an ambient atmosphere.

DOI: [10.1103/PhysRevB.97.035414](https://doi.org/10.1103/PhysRevB.97.035414)

I. INTRODUCTION

Graphene plasmons [1–6] continue to attract the interest of the scientific community, in consideration of their application capabilities [7,8]. In particular, the emergence of acoustic surface plasmons (ASP) [9–11] promises to have a superb impact on plasmonics [12–14]. ASP is a collective electronic excitation with linear dispersion on the momentum [15], previously observed on semiconductor quantum wells with interacting minibands [16] and in systems characterized by Shockley surface states (SS) [17] coexisting with bulk states, such as Be(0001) [9], Cu(111) [18–21], and Au(111) [20,22,23].

The energy of the ASP mode is

$$\omega_{\text{ASP}} = \alpha v_F^{2\text{D}} q, \quad (1)$$

where $v_F^{2\text{D}}$ is the two-dimensional (2D) Fermi velocity, q is the momentum, and α takes into account the nature of the decay and penetration of the orbitals of Shockley SS into the bulk [20].

The acoustic dispersion is originated from the joint effect of the nonlocality of the three-dimensional (3D) response and of the spill-out of the 3D electron density into the vacuum [9], which produces only partial screening of the two-dimensional (2D) electron-density oscillations. The linear dispersion relation involves the equivalence of phase and group velocities of the plasmonic excitation. Thus, in principle, signals might propagate without distortion through the surface. Consequently, the application capabilities of ASP are particularly promising [12], especially for the case of high sound

velocities of ASP modes. As a matter of fact, the observation of ASP with quasirelativistic sound velocity ($c/300$, with c being the light velocity) [10,24] in graphene (Gr) interfaced with metal gates has opened new pathways for plasmonics [12]. However, ASP does not appear in all Gr/metal interfaces. High-resolution electron-energy-loss spectroscopy (HREELS) experiments have revealed an acousticlike dispersion for Gr grown on Pt(111) [10] and Ir(111) [24], i.e., only for Gr weakly interacting with the substrate. Contrariwise, ASP is not observed in Gr/metals whenever strong hybridization of Dirac-cone electrons with metal d bands occurs, as for Gr/Ni(111) [5], for which the formation of interface states [25] induces the formation of hybridized modes localized at the Gr/Ni interface [5].

Nonlocality of screening processes in Gr [26,27] inhibits the screening of the ASP mode by the underlying metal substrate. ASP in Gr/metals represents a modification of the Dirac plasmon, supported by the 2D electron gas (2DEG) in freestanding Gr, whose dispersion in the local approximation follows [28]:

$$\omega_p = \sqrt{\frac{D}{2\varepsilon_0\varepsilon}} q. \quad (2)$$

The vacuum permittivity and the relative dielectric constant are represented in (2) by ε_0 and ε , respectively. D is the Drude weight [29], which in a 2DEG with particle density n and electron mass m_e is defined as

$$D = e^2 n / m_e, \quad (3)$$

with e the electron charge.

However, the elucidation of the emergence of ASP in Gr/metals is quite controversial [28,30,31] and a clear picture is missing yet.

*antonio.politano@iit.it

†gennaro.chiarello@fis.unical.it

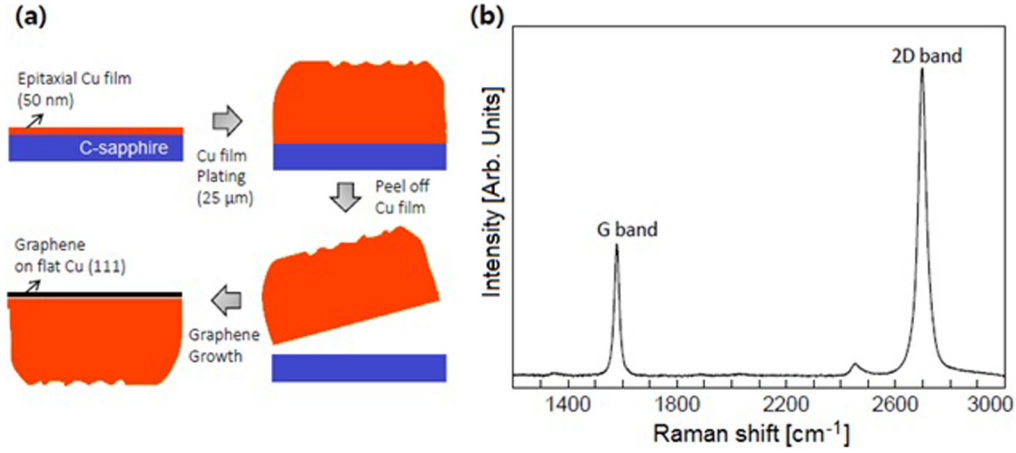


FIG. 1. (a) Schematics of the procedure for producing peeled-off epitaxial Cu(111) foils, employed as substrate for growing Gr by CVD. The Raman spectrum of the grown Gr layer is displayed in panel (b).

Gr on Cu(111) offers the possibility to probe the mutual effects of the ASP mode of Gr and that of the underlying Cu(111) substrate. Furthermore, contrarily to Pt(111) and Ir(111), Cu(111) hosts a low-energy plasmon at ~ 1 eV [32]. According to the current picture of plasmon modes in Gr/metal interfaces [33], the presence of a surface plasmon in the thick conducting substrate enables the Coulomb coupling with the Gr overlayer, with the emergence of hybrid modes. Therefore, Gr/Cu(111) represents an ideal playground to test the validity of state-of-the-art models.

The investigation of ASP in Gr/Cu(111) is further motivated by the consideration that the application capabilities of the ASP mode in Cu(111) are hindered by the oxidation of copper in ambient atmosphere [34]. In fact, surface corrosion in air, due to oxidation [35], causes ASP to disappear, as it is derived from Shockley SS [20]. On the other hand, the protection of the Cu substrate by Gr coating [36,37] might enable the exploitation in technology of the ASP mode of Shockley SS in Cu(111).

However, the growth of Gr on Cu(111) is limited to the size of a few micrometers [38] and this is a strong limitation for technological use. Differently rotated domains coexist on the surface, with a considerable degree of mosaicity [39], due to the copious number of domain boundaries. The presence of defects in Gr/Cu jeopardizes the protection of the Gr coating against corrosion of the Cu substrate via oxidation [40]. Recently, the growth of single-crystal domains of Gr as large as several hundred micrometers by means of chemical vapor deposition (CVD) on (111)-oriented Cu foils has been attained under atmospheric conditions and without wet chemical prereduction [41]. This process allows effective and easy transfer to other substrates. Gr samples obtained with this method display outstanding values of the charge-carrier mobility ($29\,000\text{ cm}^2\text{ V}^{-1}\text{ s}^{-1}$ [41]) and excellent crystalline quality of their surfaces [42].

We used these samples to investigate the excitation spectrum of Gr grown on Cu(111) foils by means of HREELS. The experimental excitation spectrum exhibits two well-distinct ASP modes, related to the Gr overlayer and to the Cu(111) substrate, respectively. While the latter plasmon mode in Gr/Cu(111) has a reduced lifetime compared to the pristine Cu(111) substrate, the Gr-related ASP is particularly suitable

for low-loss plasmonics, due to its higher lifetime compared to any other Gr/metal interface.

II. EXPERIMENTAL METHODS

Spectroscopic investigations have been performed in an ultrahigh vacuum (UHV) chamber working at a base pressure of 4×10^{-9} Pa. Gr was grown on a Cu foil using the procedure reported in Ref. [41]. The basic steps involved are schematically shown in Fig. 1(a). Primarily, an epitaxial Cu(111) film of several tens of nanometers is grown on the C-plane sapphire by electron-beam evaporation and additional tens of micrometers of Cu layers are deposited by electrochemical methods. Due to an appropriate (8.6%) lattice mismatch between C-plane sapphire and Cu(111), the Cu film is successively effortlessly peeled away from the sapphire substrate. The side of the foil formerly touching the sapphire is the one employed in catalytic CVD Gr growth. This process was carried out in a quartz tube reaction chamber, by means of methane gas at a growth temperature of 1000°C . Additional information on the Gr growth process is reported in Ref. [41].

The Raman spectra were acquired with a LabRAM HR 800 spectrometer with an excitation wavelength of 633 nm.

HREELS experiments have been carried out at room temperature by using an electron-energy-loss spectrometer (Delta 0.5, SPECS) with an angular acceptance of $\pm 0.5^\circ$. The energy resolution of the spectrometer has been degraded to 3 meV, so as to increase the signal-to-noise ratio of loss peaks. Angle-resolved HREELS experiments have been carried out by moving the analyzer with the sample and the monochromator in a fixed position. A polynomial background has been subtracted from each spectrum.

By considering the conservation laws of energy and momentum (see reviews in Refs. [43,44]), it is possible to evaluate the parallel momentum transfer q_{\parallel} from kinematic conditions and from the loss energy E_{loss} :

$$q_{\parallel} = \frac{\sqrt{2mE_p}}{\hbar} \left(\sin \theta_i - \sqrt{1 - \frac{E_{\text{loss}}}{E_p}} \sin \theta_s \right), \quad (4)$$

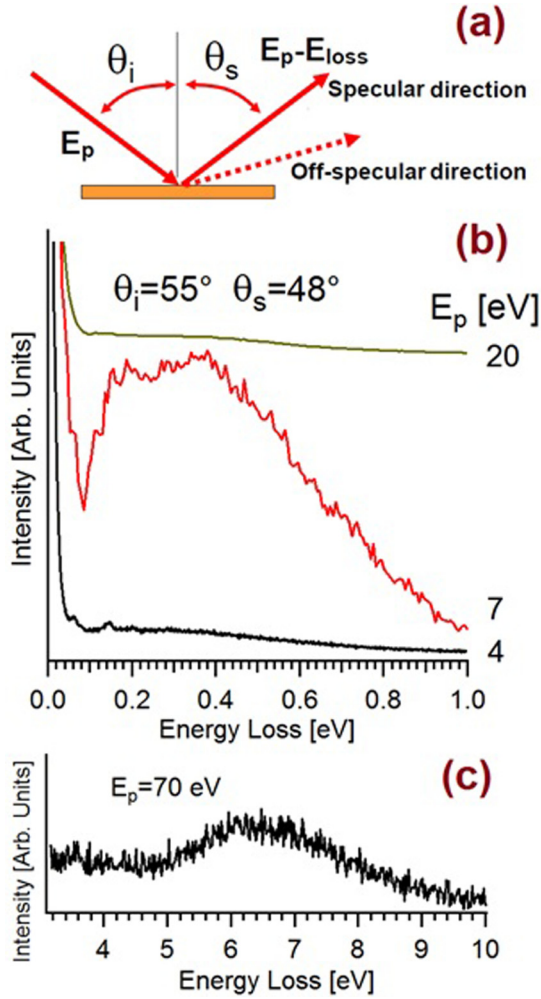


FIG. 2. (a) HREELS scattering geometry. Panels (b,c) display the excitation spectrum probed by HREELS for various values of the impinging energy, at fixed scattering conditions. In details, in panel (b) the 0–1 eV energy range is shown, while in panel (c) the range of the interband plasmon is shown.

where θ_i and θ_s are the incidence and final scattering angle with respect to the surface normal, respectively [see Fig. 2(a) for a sketch].

The indeterminacy in the momentum domain Δq_{\parallel} , which depends also on the angular acceptance of the apparatus δ [44], is estimated to be

$$\Delta q_{\parallel} = \frac{\sqrt{2mE_p}}{\hbar} \left(\cos \theta_i + \sqrt{1 - \frac{E_{\text{loss}}}{E_p}} \cos \theta_s \right) \delta. \quad (5)$$

III. RESULTS AND DISCUSSION

A typical Raman spectrum of Gr grown on a peeled-off epitaxial Cu(111) foil is shown in Fig. 1(b). The superb crystalline quality of monolayer Gr is proven by the symmetric 2D band and, moreover, by the 2D line twice more intense than the G line ($I_{2D}/I_G = 2$).

Detecting ASP excitations with electron probes requires a careful tuning of the kinetic energy of impinging electrons in order to maximize the signal coming from ASP. For this reason,

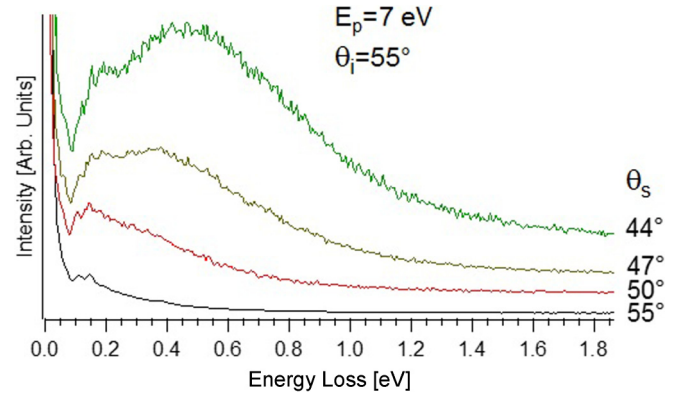


FIG. 3. Momentum-resolved EELS spectra recorded in a 0–1.9-eV range of loss energies. The primary electron-beam energy is 7 eV.

we have investigated the behavior of the excitation spectrum as a function of the primary electron-beam energy E_p at fixed scattering conditions. In Fig. 2(b), we show spectra recorded at various values of E_p . Intense and well-distinct peaks are evident in the loss spectrum only at $E_p = 7$ eV. By analyzing their linewidth and energy position, as well as their behavior with the momentum, we can exclude their vibrational nature and we ascribe them to plasmonic modes. At higher values of E_p , the loss spectrum is dominated by interband π plasmons at loss energies around 7 eV [45] [see the spectrum in Fig. 2(c), acquired at $E_p = 70$ eV].

Such a singular behavior of the loss function is merely typical of ASP modes. As a matter of fact, also for the case of pristine Cu(111), ASP is visible only at the lowest values of E_p [19,21], while at $E_p = 20$ eV its intensity is vanishing [32].

Figure 3 reports the momentum-resolved EELS spectra of Gr on Cu(111) in the spectral region of the intraband plasmon with $E_p = 7$ eV. The loss spectrum in specular geometry is characterized by a single peak. In off-specular spectra, another feature emerges and becomes the predominant peak for a scattering angle of 47°.

It is also worth noticing that the intensity of plasmonic losses increases with the off-specular angle and, correspondingly, with the momentum. In particular, the behavior of the intensity of the peak associated with the plasmonic mode as a function of the momentum represents an indicator of the plasmon lifetime. As a matter of fact, the decay of plasmon modes in electron-hole pairs has effects not only on the linewidth [46,47], but also on the intensity of the plasmonic excitation.

For the cases of Gr on Pt(111) [48] and Ni(111) [5], the intensity of the intraband plasmon has been found to decrease beyond a critical wave vector $q_c = 0.12 \text{ \AA}^{-1}$ (Supplemental Material [49], Fig. S1). In Gr on SiC(0001) [50] and Ir(111) [24], the critical wave vector q_c is reduced to 0.08 and $\sim 0.07 \text{ \AA}^{-1}$, respectively. Conversely, in Gr/Cu(111), we find a monotonous increase of both plasmonic losses as a function of momentum, even at $q > 0.2 \text{ \AA}^{-1}$. This finding should be related to the weak (though existing) hybridization of Gr π states and d bands of Cu(111) [51], which implies the opening of a band gap of ~ 19 meV [51], caused by spin-orbit

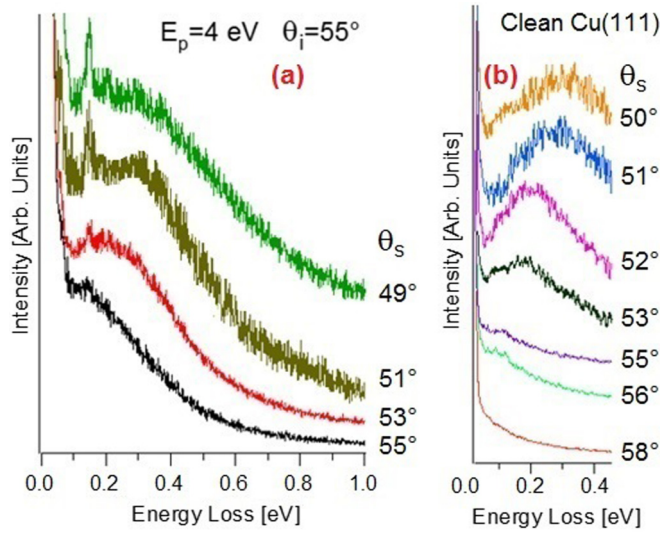


FIG. 4. HREELS spectra of (a) Gr/Cu(111) and (b) pristine Cu(111), acquired at $E_p = 4$ eV as a function of the scattering angle.

proximity effects [51]. The presence of a band gap leads to an extended region of undamped propagation of ASP of Gr in the momentum domain, as previously found for the intraband plasmon of Gr in both gapped freestanding Gr [52] and Gr interfaced with a thick conductor [33]. Moreover, it has been demonstrated that, if the Gr-substrate distance h is less than a critical value $d \sim 0.4k_F^{-1}$ (with k_F the Fermi wave vector), the lower ASP mode is overdamped near $q = 0$ [53]. In Gr/Cu(111), the Gr-metal distance is $\sim 3.2 \text{ \AA}$ [54] and $k_F = 0.15 \text{ \AA}^{-1}$ [55]. Hence, as $h > d$, ASP in Gr/Cu(111) is expected to propagate in a regime characterized by reduced Landau damping, provided that the step density of the Gr sample is sufficiently low [56], i.e., a condition satisfied by our samples with a scarce amount of defects, as also certified by previous helium-atom scattering experiments on the same samples [42].

The analysis of Fig. 3 clarifies that two different excitations exist in the Gr/Cu(111) system. The feature at higher energy is evidently associated with the ASP mode in Gr. Concerning the mode at lower energy, an accurate analysis of the dispersion relation of the low-energy mode indicates that it can be related to the ASP mode of the underlying Cu(111) substrate. The detection of a subsurface mode with a spectroscopic tool based on reflection of incoming probes is rather challenging. In principle, HREELS can probe a subsurface excitation [57,58]. However, subsurface charge-density oscillations can be revealed only at specific values of the impinging energy, for which the reflection plane at which electrons are scattered lies in the subsurface region [59]. Thus, in order to increase the cross section for the excitation of plasmonic modes underneath the Gr cover, the primary electron-beam energy has been decreased to 4 eV. As a matter of fact, the mean free path for impinging electrons at that value of the kinetic energy [60] is sufficient to enable the detection of collective excitations located in the subsurface region. The loss function recorded at $E_p = 4$ eV [Fig. 4(a)] shows a single plasmonic excitation with an acoustic dispersion, superimposed with sharp peaks

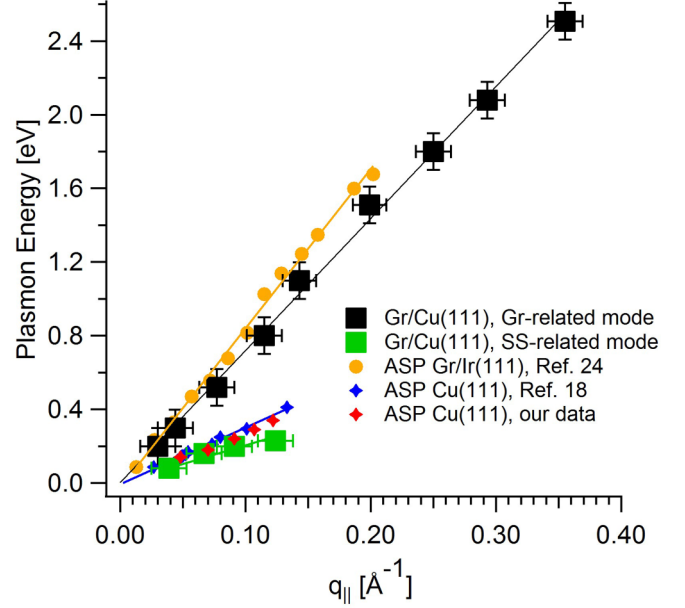


FIG. 5. Dispersion relation of Gr/Cu(111) (black and green squares for the two ASP modes), Gr/Ir(111) (orange circles, data taken from Ref. [24]), and the pristine Cu(111) (red diamonds for our data and blue diamonds for data taken from Ref. [18], respectively).

emerging in off-specular spectra, which are related to phonon modes [61] of the Gr/Cu(111) interface. The dispersion relation of this mode (shown in Fig. 5) is quite similar to that reported by Pischel *et al.* for ASP in Cu(111) [18]. In Fig 4(b), HREELS spectra that we acquired for pristine Cu(111) foils as a function of the scattering angle are reported. A direct comparison of data in Figs. 4(a) and 4(b) with the dispersion relation in Fig. 5 could be a straightforward way to evidence the effects of the presence of Gr on (i) the lifetime and (ii) the dispersion relation of the ASP of Cu(111).

An evident difference is related to the attenuation of ASP of Cu(111) in the presence of the Gr cover. However, it should be considered that HREELS operates in reflection modality [62]. This implies that the vacuum/Gr interface has higher spectral weight in the experimental excitation spectrum compared to the Gr/Cu interface. Therefore, it is trivial that subsurface excitations are naturally attenuated when probed with reflection HREELS.

The lifetime of the mode at lower energy is reduced in Gr/Cu(111) with respect to the case of pristine Cu(111), as revealed by a direct comparison (Supplemental Material [49], Fig. S2). This is a consequence of the hybridization of Gr π states and d bands of Cu(111) [51] that, albeit weak, does exist.

By analyzing the dispersion relation in Fig. 5, it is also manifest that the dispersion of the Gr-related mode ASP in Gr/Cu(111) is considerably ($\sim 14\%$) less steep compared to Gr/Ir(111) [24]. However, a comparison of the ASP in Gr/Cu(111) with that previously measured by us for Gr/Pt(111) [10] indicates a substantially similar dispersion.

The comparison of the sound velocity v of the ASP to the Fermi velocity of the SS v_{SS} can provide important information on the screening process. The $\alpha = v/v_{SS}$ ratio is higher than 1 if the majority of the bulk electrons with energies around the

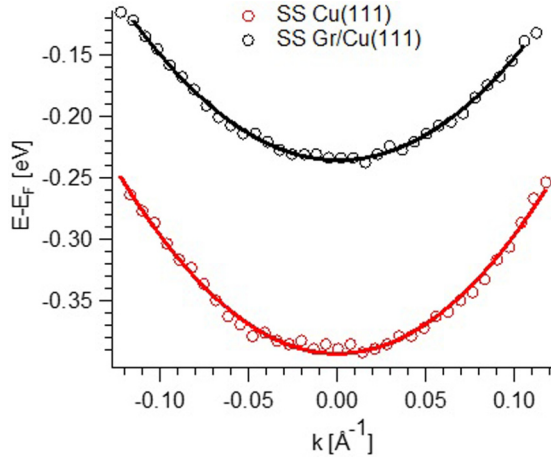


FIG. 6. Dispersion relation of Shockley SS in Cu(111) and Gr/Cu(111) (data taken from Ref. [63]).

Fermi level move quicker with respect to SS electrons [18]. Conversely, for $\alpha < 1$ screening of most of the slowly moving bulk electrons is given by the faster electrons of the SS. As an example, $\alpha = 0.8$ in the case of Au(111) [23].

We have also evaluated the sound velocity of the ASP in clean Cu(111), finding $v_{\text{Cu}} = (2720 \pm 250) \text{ meV } \text{\AA}$. This value is lower than that reported by Pischel *et al.* [18] ($\sim 3100 \text{ meV } \text{\AA}$), even if the two values are comparable, if considering the experimental inaccuracy.

The ASP sound velocity for Cu(111) can be compared to the Fermi velocity of Shockley SS on Cu(111) ($3825 \text{ meV } \text{\AA}$ [11]). The ratio is $\alpha = 0.71 < 1$. This implies that the ASP disperses into the continuum of electron-hole pairs within the SS, in agreement with the interpretation by Pischel *et al.* [18]. Therefore, it can be concluded that, in agreement with the model devised for Au(111) [23], also in Cu(111) most of the bulk electrons with energies around the Fermi level move slower than the electrons of the Shockley SS. Thus, the plasmonic resonance should be associated to the screening of bulk electrons by electrons of the SS rather than the reverse.

A similar analysis can be carried out for the two ASP excitations in Gr/Cu(111). We find the sound velocities to be $v_1 = (7180 \pm 76)$ and $v_2 = (2041 \pm 120) \text{ meV } \text{\AA}$.

Firstly, we note that the sound velocity of ASP in Cu(111) is decreased in the presence of Gr ($v_2 < v_{\text{Cu}}$). It should be considered that the Cu(111) Shockley SS are shifted by 0.15 eV toward the Fermi energy in the presence of Gr [63] (Fig. 6), due to the charge transfer at the Gr/Cu interface activated by the different work functions of Gr and Cu(111) [64].

A careful analysis of angle-resolved photoemission spectroscopy (ARPES) data in Ref. [63] also evidences a slight increase of the effective mass of electrons in Shockley SS. As a matter of fact, a fit procedure to the dispersion of the SS measured by ARPES with a parabolic line shape (Fig. 6) indicates that the quadratic coefficient of the parabola decreases by 12% in Gr/Cu(111). The subsequent increase of the effective mass in Gr/Cu(111) implies a less steep dispersion of the v_2 mode compared to pristine Gr/Cu(111), in excellent agreement with the experimental findings in Fig. 5.

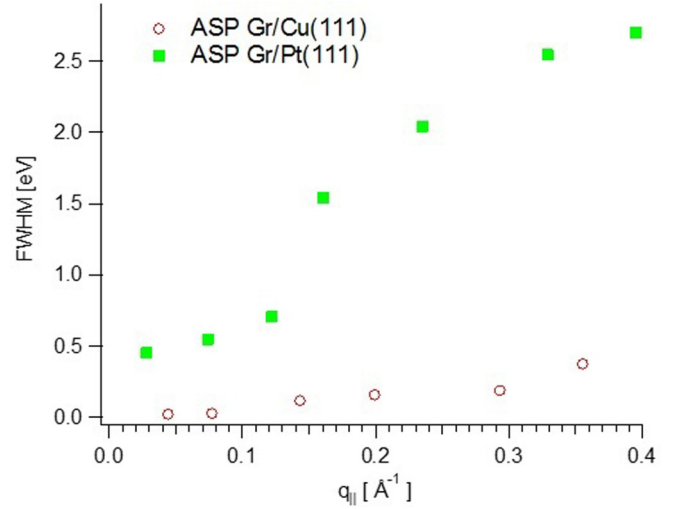


FIG. 7. Behavior of the FWHM for the ASP peak in Gr/Cu(111) (empty red circles) and Gr/Pt(111) (filled green squares) as a function of momentum.

Remarkably, we note that the sound velocity v_1 coincides, within the experimental inaccuracy, with the value of the slope of the Dirac cone in Gr/Cu(111) extrapolated by the fitting of the Dirac-cone dispersion in Ref. [63], i.e., $(7032 \pm 220) \text{ meV } \text{\AA}$. Therefore, we can unambiguously ascribe the mode with sound velocity v_1 to the undamped ASP of Dirac-cone electrons in Gr/Cu(111). For the sake of comparison, in the case of ASP in Gr/Ir(111) we evaluate the sound velocity $v_{\text{Gr-Ir}}$ to be $(8200 \pm 500) \text{ meV } \text{\AA}$ [24]. Similarly, for ASP in Gr/Pt(111) the sound velocity is $v_{\text{Gr-Pt}} (7400 \pm 100) \text{ meV } \text{\AA}$ [10].

The quantitative estimation of the lifetime of a plasmonic mode by HREELS is not straightforward, because of the contribution of different effects, which broaden the experimental linewidth. Nevertheless, the comparative evaluation of the variations of the full width at half maximum (FWHM) for the ASP peak in different Gr/metal interfaces could provide important information on the damping processes. In Fig. 7, we compare the momentum dependence of FWHM of the ASP peak in the HREELS spectrum in Gr/Cu(111) and Gr/Pt(111) in the same scattering conditions and with the same experimental configuration of the spectrometer. It is evident that the FWHM of ASP in Gr/Cu(111) is reduced by one order of magnitude compared to Gr/Pt(111); the subsequent implication is that the ASP lifetime is about ten times higher in Gr/Cu(111). We also note that in both cases the FWHM increases after a critical momentum of about 0.15 \AA^{-1} , because of the opening of decay channels of the ASP in electron-hole pairs.

For practical exploitation of ASP in technology, the assessment of the stability of the plasmonic mode in air-exposed samples is crucial. Unfortunately, the ASP of Cu(111) is totally quenched in Cu samples exposed to ambient atmosphere, i.e., the signal from ASP in air-exposed samples is null. This finding can be explained by considering that Shockley SS of Cu(111), which originate ASP [19,20], are absent for oxidized Cu(111) [35]. Corrosion of copper in air is unavoidable due to the dehydration process occurring during wet-dry and cold-hot

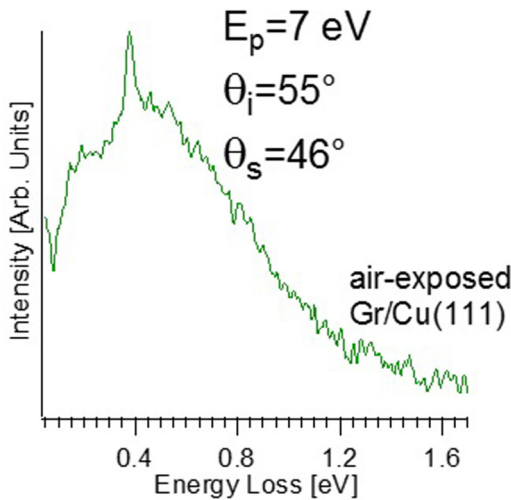


FIG. 8. Typical excitation spectrum in air-exposed Gr/Cu(111). Together with the two ASP modes, the C-H stretching at 0.37 eV is observed.

cycles [65]. Such processes are enhanced in atmospheres with particulate matter [66]. However, Gr coating inhibits copper oxidation [36]. In the air-exposed Gr/Cu(111) contact, both ASP modes survive, as shown in Fig. 8. The unique noticeable change compared to the pristine Gr/Cu(111) is the presence of C-H groups arising from water decomposition at room temperature [67], evidenced by the C-H stretching at 0.37 eV

[67], together with a general attenuation of the HREELS signal, due to the adsorbed water fragments.

IV. CONCLUSIONS

We have studied the excitation spectrum of Gr epitaxially grown on Cu(111) foils. The loss spectrum, probed by EELS, is characterized by two ASP modes. The mode at lower energy arises from Cu(111) Shockley SS. It survives, even if shifted and with higher effective mass, in the Gr/Cu(111) substrate. The plasmon at higher energy is originated from Dirac-cone electrons: its group velocity coincides with the slope of the Dirac cone and it is undamped in the weakly interacting Gr/Cu(111) interface. We have also demonstrated that the ASP modes in Gr/Cu(111) are resistant toward ambient atmosphere. On the basis of experimental results, one can endorse Gr/Cu as a suitable Gr/metal contact for viable low-loss plasmonics based on Gr.

ACKNOWLEDGMENTS

A.P. and G.C. thank Fabio Vito for technical support. D.F. acknowledges financial support from the Spanish MINECO under Project No. MAT2015-65356-C3-3-R (MINECO/FEDER) and through the “Maria de Maeztu” Programme for Units of Excellence in R&D (Program No. MDM-2014-0377). We thank Mikkel Strange and Kristian S. Thygesen for helpful discussions.

- [1] M. M. Jadidi, J. C. König-Otto, S. Winnerl, A. B. Sushkov, H. D. Drew, T. E. Murphy, and M. Mittendorff, *Nano Lett.* **16**, 2734 (2016).
- [2] J. D. Cox, I. Silveiro, and F. J. García De Abajo, *ACS Nano* **10**, 1995 (2016).
- [3] P. Alonso-González, A. Y. Nikitin, F. Golmar, A. Centeno, A. Pesquera, S. Vélez, J. Chen, G. Navickaite, F. Koppens, A. Zurutuza, F. Casanova, L. E. Hueso, and R. Hillenbrand, *Science* **344**, 1369 (2014).
- [4] A. Cupolillo, N. Ligato, and L. S. Caputi, *Appl. Phys. Lett.* **102**, 111609 (2013).
- [5] A. Cupolillo, N. Ligato, and L. Caputi, *Surf. Sci.* **608**, 88 (2013).
- [6] A. Cupolillo, N. Ligato, and L. S. Caputi, *Carbon* **50**, 2588 (2012).
- [7] X. Lin, Y. Yang, N. Rivera, J. J. López, Y. Shen, I. Kaminer, H. Chen, B. Zhang, J. D. Joannopoulos, and M. Soljačić, *Proc. Natl. Acad. Sci. U.S.A.* **114**, 6717 (2017).
- [8] X. Lin, I. Kaminer, X. Shi, F. Gao, Z. Yang, Z. Gao, H. Buljan, J. D. Joannopoulos, M. Soljačić, H. Chen, and B. Zhang, *Sci. Adv.* **3**, e1601192 (2017).
- [9] B. Diaconescu, K. Pohl, L. Vattuone, L. Savio, P. Hofmann, V. M. Silkin, J. M. Pitarke, E. V. Chulkov, P. M. Echenique, D. Farías, and M. Rocca, *Nature* **448**, 57 (2007).
- [10] A. Politano, A. R. Marino, V. Formoso, D. Farías, R. Miranda, and G. Chiarello, *Phys. Rev. B* **84**, 033401 (2011).
- [11] J. Yan, K. W. Jacobsen, and K. S. Thygesen, *Phys. Rev. B* **86**, 241404 (2012).
- [12] P. Alonso-González, A. Y. Nikitin, Y. Gao, A. Woessner, M. B. Lundberg, A. Principi, N. Forcellini, W. Yan, S. Vélez, A. J. Huber, K. Watanabe, T. Taniguchi, F. Casanova, L. E. Hueso, M. Polini, J. Hone, F. H. L. Koppens, and R. Hillenbrand, *Nat. Nanotechnol.* **12**, 31 (2017).
- [13] Q. Zhu, F. Qin, J. Lu, Z. Zhu, H. Nan, Z. Shi, Z. Ni, and C. Xu, *Nano Res.* **10**, 1996 (2017).
- [14] B. Park, S. J. Kim, J. S. Sohn, M. S. Nam, S. Kang, and S. C. Jun, *Nano Res.* **9**, 1866 (2016).
- [15] J.-K. Ahn, Y.-I. Kim, K.-H. Kim, C.-J. Kang, M. C. Ri, and S.-H. Kim, *Phys. B (Amsterdam, Neth.)* **481**, 257 (2016).
- [16] M. T. Bootsmann, C. M. Hu, C. Heyn, D. Heitmann, and C. Schüller, *Phys. Rev. B* **67**, 121309 (2003).
- [17] A. Tamai, W. Meevasana, P. D. C. King, C. W. Nicholson, A. de la Torre, E. Rozbicki, and F. Baumberger, *Phys. Rev. B* **87**, 075113 (2013).
- [18] J. Pischel, E. Welsch, O. Skibbe, and A. Pucci, *J. Phys. Chem. C* **117**, 26964 (2013).
- [19] K. Pohl, B. Diaconescu, G. Vercelli, L. Vattuone, V. M. Silkin, E. V. Chulkov, P. M. Echenique, and M. Rocca, *Europhys. Lett.* **90**, 57006 (2010).
- [20] V. M. Silkin, J. M. Pitarke, E. V. Chulkov, and P. M. Echenique, *Phys. Rev. B* **72**, 115435 (2005).
- [21] L. Vattuone, G. Vercelli, M. Smerieri, L. Savio, and M. Rocca, *Plasmonics* **7**, 323 (2012).
- [22] S. J. Park and R. E. Palmer, *Phys. Rev. Lett.* **105**, 016801 (2010).

- [23] L. Vattuone, M. Smerieri, T. Langer, C. Tegenkamp, H. Pfnür, V. M. Silkin, E. V. Chulkov, P. M. Echenique, and M. Rocca, *Phys. Rev. Lett.* **110**, 127405 (2013).
- [24] T. Langer, D. F. Förster, C. Busse, T. Michely, H. Pfnür, and C. Tegenkamp, *New J. Phys.* **13**, 053006 (2011).
- [25] S. D. Yu and M. Fonin, *New J. Phys.* **12**, 125004 (2010).
- [26] J. Yan, K. S. Thygesen, and K. W. Jacobsen, *Phys. Rev. Lett.* **106**, 146803 (2011).
- [27] M. van Schilfgaarde and M. I. Katsnelson, *Phys. Rev. B* **83**, 081409 (2011).
- [28] T. Stauber, *J. Phys.: Condens. Matter* **26**, 123201 (2014).
- [29] S. H. Abedinpour, G. Vignale, A. Principi, M. Polini, W.-K. Tse, and A. H. MacDonald, *Phys. Rev. B* **84**, 045429 (2011).
- [30] N. J. M. Horing, *Phys. Rev. B* **80**, 193401 (2009).
- [31] N. J. M. Horing, *IEEE Trans. Nanotechnol.* **9**, 679 (2010).
- [32] A. Politano, G. Chiarello, V. Formoso, R. G. Agostino, and E. Colavita, *Phys. Rev. B* **74**, 081401 (2006).
- [33] G. Gumbs, A. Iurov, and N. J. M. Horing, *Phys. Rev. B* **91**, 235416 (2015).
- [34] K. P. Fitzgerald, J. Nairn, G. Skennerton, and A. Atrens, *Corros. Sci.* **48**, 2480 (2006).
- [35] S. Gottardi, K. Müller, L. Bignardi, J. C. Moreno-López, T. A. Pham, O. Ivashenko, M. Yablonskikh, A. Barinov, J. Björk, and P. Rudolf, *Nano Lett.* **15**, 917 (2015).
- [36] D. Prasai, J. C. Tuberquia, R. R. Harl, G. K. Jennings, and K. I. Bolotin, *ACS Nano* **6**, 1102 (2012).
- [37] S. Chen, L. Brown, M. Levendoff, W. Cai, S.-Y. Ju, J. Edgeworth, X. Li, C. W. Magnuson, A. Velamakanni, R. D. Piner, J. Kang, J. Park, and R. S. Ruoff, *ACS Nano* **5**, 1321 (2011).
- [38] L. Gao, J. R. Guest, and N. P. Guisinger, *Nano Lett.* **10**, 3512 (2010).
- [39] S. Nie, J. M. Wofford, N. C. Bartelt, O. D. Dubon, and K. F. McCarty, *Phys. Rev. B* **84**, 155425 (2011).
- [40] I. Wlasny, P. Dabrowski, M. Rogala, P. Kowalczyk, I. Pasternak, W. Strupinski, J. Baranowski, and Z. Klusek, *Appl. Phys. Lett.* **102**, 111601 (2013).
- [41] H. K. Yu, K. Balasubramanian, K. Kim, J.-L. Lee, M. Maiti, C. Ropers, J. Krieg, K. Kern, and A. M. Wodtke, *ACS Nano* **8**, 8636 (2014).
- [42] A. Al Taleb, H. K. Yu, G. Anemone, D. Farías, and A. M. Wodtke, *Carbon* **95**, 731 (2015).
- [43] A. Politano and G. Chiarello, *Prog. Surf. Sci.* **90**, 144 (2015).
- [44] M. Rocca, *Surf. Sci. Rep.* **22**, 1 (1995).
- [45] A. Politano, I. Radović, D. Borka, Z. L. Mišković, H. K. Yu, D. Farías, and G. Chiarello, *Carbon* **114**, 70 (2017).
- [46] V. M. Silkin, E. V. Chulkov, and P. M. Echenique, *Phys. Rev. Lett.* **93**, 176801 (2004).
- [47] Z. Yuan and S. Gao, *Surf. Sci.* **602**, 460 (2008).
- [48] A. Politano and G. Chiarello, *Carbon* **71**, 176 (2014).
- [49] See Supplemental Material at <http://link.aps.org/supplemental/10.1103/PhysRevB.97.035414> for additional information on (i) the behavior of the intensity of the intraband plasmon in different Gr/metal interfaces as a function of the momentum, and (ii) the comparison of the line shape of the ASP for Cu(111) and Gr/Cu(111) for a selected value of the momentum.
- [50] Y. Liu, R. F. Willis, K. V. Emtsev, and T. Seyller, *Phys. Rev. B* **78**, 201403 (2008).
- [51] T. Frank, M. Gmitra, and J. Fabian, *Phys. Rev. B* **93**, 155142 (2016).
- [52] P. K. Pyatkovskiy, *J. Phys.: Condens. Matter* **21**, 025506 (2009).
- [53] G. Gumbs, A. Iurov, J.-Y. Wu, M. F. Lin, and P. Fekete, *Sci. Rep.* **6**, 21063 (2016).
- [54] G. Giovannetti, P. A. Khomyakov, G. Brocks, V. M. Karpan, J. van den Brink, and P. J. Kelly, *Phys. Rev. Lett.* **101**, 026803 (2008).
- [55] A. L. Walter, S. Nie, A. Bostwick, K. S. Kim, L. Moreschini, Y. J. Chang, D. Innocenti, K. Horn, K. F. McCarty, and E. Rotenberg, *Phys. Rev. B* **84**, 195443 (2011).
- [56] T. Langer, J. Baringhaus, H. Pfnür, H. W. Schumacher, and C. Tegenkamp, *New J. Phys.* **12**, 033017 (2010).
- [57] A. Politano, A. R. Marino, and G. Chiarello, *Chem. Phys.* **367**, 148 (2010).
- [58] L. Vattuone, L. Savio, and M. Rocca, *Phys. Rev. Lett.* **90**, 228302 (2003).
- [59] V. U. Nazarov, *Phys. Rev. B* **59**, 9866 (1999).
- [60] M. Seah and W. Dench, *Surf. Interface Anal.* **1**, 2 (1979).
- [61] A. Al Taleb and D. Farías, *J. Phys.: Condens. Matter* **28**, 103005 (2016).
- [62] H. Ibach and D. L. Mills, *Electron Energy Loss Spectroscopy and Surface Vibrations* (Academic Press, San Francisco, 1982).
- [63] C. Jeon, H.-N. Hwang, W.-G. Lee, Y. G. Jung, K. S. Kim, C.-Y. Park, and C.-C. Hwang, *Nanoscale* **5**, 8210 (2013).
- [64] S. Pagliara, S. Tognolini, L. Bignardi, G. Galimberti, S. Achilli, M. I. Trioni, W. F. van Dorp, V. Ocelík, P. Rudolf, and F. Parmigiani, *Phys. Rev. B* **91**, 195440 (2015).
- [65] D. C. Kong, C. F. Dong, Y. H. Fang, K. Xiao, C. Y. Guo, G. He, and X. G. Li, *J. Mater. Eng. Perform.* **25**, 2977 (2016).
- [66] H. Gil, C. P. Buitrago, and J. A. Calderón, *J. Solid State Electrochem.* **21**, 1111 (2017).
- [67] A. Politano, M. Cattelan, D. W. Boukhalov, D. Campi, A. Cupolillo, S. Agnoli, N. G. Apostol, P. Lacovig, S. Lizzit, D. Farías, G. Chiarello, G. Granozzi, and R. Larciprete, *ACS Nano* **10**, 4543 (2016).